RAPID COMMUNICATIONS

PHYSICAL REVIEW B VOLUME 36, NUMBER 4 1 AUGUST 1987

Free-carrier relaxation dynamics in the normal state of sintered $YBa_2Cu_3O_{7-y}$

P. E. Sulewski, T. W. Noh, J. T. McWhirter, and A. J. Sievers
Laboratory of Atomic and Solid State Physics and Materials Science Center, Cornell University, Ithaca, New York 14853-2501

S. E. Russek and R. A. Buhrman
School of Applied and Engineering Physics and Materials Science Center, Cornell University, Ithaca, New York 14853-2501

C. S. Jee, J. E. Crow, R. E. Salomon, and G. Myer
Department of Physics, Temple University, Philadelphia, Pennsylvania 19122
(Received 22 May 1987)

The conductivity of $YBa_2Cu_3O_{7-y}$ in the normal state has been obtained from a measurement of the reflectivity over a wide frequency range. The product of the Drude model parameters $\omega_p\tau < 1$ indicates that the plasma oscillations are overdamped. The free-carrier electrodynamics are well described by a frequency-dependent scattering rate which rises linearly in frequency from the dc value and saturates at a value consistent with scattering at the unitarity limit with a concomitant frequency-dependent mass enhancement.

A number of theoretical explanations[1-4] for the high superconducting transition temperature of the La and Y copper oxide ceramics start from an assumption of the two-dimensional (2D) character of a nearly-half-filled copper oxide band. While some[1] of the mechanisms proposed do not depend on this 2D character, others depend critically on,[2,3] or at least are favored[4] by the 2D character of the electrons. The insensitivity of the T_c to substitution of Y with a number of rare earths, including Gd and Ho,[5] provides additional evidence for the 2D nature of the charge carriers. Also, several band-structure calculations[6,7] show that the electron density is highly constrained to the 2D Cu-O planes. A hallmark of strongly 2D coupled conduction carriers in such a model is that both the relaxation time and the carrier mass[8-10] are frequency dependent but with a dependence different from that found for 3D systems; namely, the inverse relaxation time varies linearly with frequency and the carrier mass shows a logarithmic singularity at zero frequency.

To test this 2D possibility we have measured the far-infrared (FIR) reflectivity of sintered $YBa_2Cu_3O_{7-y}$ in the normal state between 100 K and room temperature over a large frequency interval, obtained the real and imaginary parts of the frequency dependent conductivity from a Kramers-Kronig analysis, and then separated out the free-carrier contribution from the phonon and bound-carrier ones. Our experimental results and analysis demonstrate that the effective relaxation frequency and mass of the conduction carriers do show the frequency dependences expected for 2D behavior.

Polycrystalline samples of $YBa_2Cu_3O_{7-y}$ were prepared by solid-state reaction of Y_2O_3, CuO, and $BaCO_3$, all of 99.999% purity. X-ray diffraction measurements demonstrated single-phase samples, with the structure reported in the literature.[11] Scanning electron micrographs (SEM) of the polished samples reveal the presence of pits or voids with a characteristic size of ~ 10 μm. By measuring the density of the samples, we can calculate the porosity, which is about 25%, in agreement with the value obtained from the SEM estimate. Between the voids, the surface is mirror quality, smooth to the $\sim$500-Å scale. Reflectivity measurements on these samples span four decades in frequency, from 4 to 40000 cm^{-1} (0.5 meV–5 eV).[12]

The room-temperature FIR reflectivity of $YBa_2Cu_3O_{7-y}$ is represented by the solid line in Fig. 1(a). Also shown in this figure (dashed line) is the classical skin effect prediction for a dc resistivity of 800 $\mu\Omega$ cm (the measured resistivity is $890 \pm 10\%$ $\mu\Omega$ cm). At the lowest-frequency limit of our data the two curves converge, but for higher frequencies, the reflectivity deviates strongly from the Drude prediction. We also observe very little temperature dependence to the reflectivity (100 K, dotted line) in agreement with other measurements at larger frequencies.[13] While the dc resistivity changes by a factor of 3,[11] from just above T_c to room temperature the reflectivity changes by only a few percent.

Figure 1(b) shows the room-temperature reflectivity as a function of frequency on a logarithmic frequency axis, covering four decades in frequency. The appearance of phonon modes such as those shown in the 100-to-1000-cm^{-1} region is not common in metallic reflectivity, but in materials with small optical conductivity their observability has been confirmed both experimentally[14] and theoretically.[15]

Since the samples have a porosity of approximately 25%, a detailed interpretation of the optical reflectivity is lacking, requiring a geometric correction for voids, with a characteristic size l, at wavelengths $\lambda \ll l$, and an effective medium approach for $\lambda \gg l$. Even so, performing a Kramers-Kronig analysis of the reflectivity data to obtain the effective complex conductivity in the low-frequency

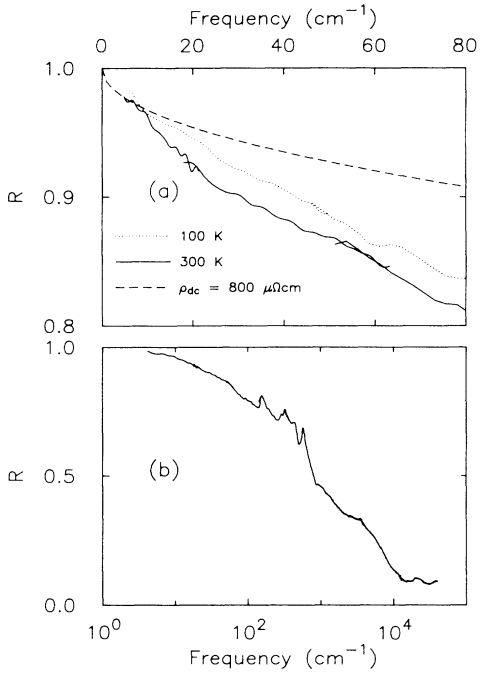

FIG. 1. Normal incidence reflectivity of $YBa_2Cu_3O_{7-y}$ as a function of frequency. (a) Solid curves show the room-temperature reflectivity below 80 cm^{-1}. Dotted curve shows data at 100 K. Dashed curve is the calculated classical skin effect value for the reflectivity determined from a dc resistivity of 800 $\mu\Omega$ cm. (b) Room-temperature reflectivity measured over four decades, shown on a logarithmic frequency axis.

limit is a useful first step to characterize the material. Theoretical studies of the optical properties of composites[16] demonstrate that generalized sum rules obeyed by the effective dielectric function can provide limits on important quantities such as the plasma frequency.

In order to obtain the complex conductivity for this sample, we perform a Kramers-Kronig analysis of our composite reflectivity. Since, as shown in Fig. 1(a), the Drude prediction with a dc resistivity of 800 $\mu\Omega$ cm matches onto the data, we use this extrapolation to zero frequency to obtain the curves which follow. At the high-frequency end, since our uv data show a relatively constant reflectivity, indicative of a constant ϵ_∞, the curves shown here are obtained by extrapolating the reflectivity with a constant.

For traditional conductors, the standard analysis to obtain the value of ω_p relies on determining the zero of ϵ_1 or the pole of $-\mathrm{Im}\epsilon^{-1}$. These two functions for $YBa_2Cu_3O_{7-y}$ are shown in Fig. 2, as the solid and dashed curve, respectively. Ignoring the detailed structure, the figure clearly shows that the two standard signatures of ω_p are separated by over an order of magnitude in frequency, and hence the plasma frequency cannot be obtained directly by inspection.

The complex conductivity obtained from the Kramers-Kronig transformation is shown in Fig. 3. The imaginary component, shown as the dashed curve, has been calculated assuming a value of 3.7 for the dielectric constant ϵ_∞. Phonon peaks[17] which occur in the range of 100–1000 cm^{-1} are visible owing to the small magnitude of the free-carrier conductivity in this frequency range. Two interband peaks are identified and their center frequencies are given in Table I. All of this structure appears superimposed on a constant background conductivity due to free carriers.

Below 100 cm^{-1} the real part of the conductivity shown in Fig. 3 has a constant value, until about 10 cm^{-1}, where it begins to rise to the dc value. This rise occurs independently on the dc resistivity used in the low-frequency extrapolation of the reflectivity. We find that the position of this initial rise in the low-frequency conductivity is controlled by the measured frequency dependence of the FIR reflectivity data which extended down to 4 cm^{-1} as shown in Fig. 1(a).

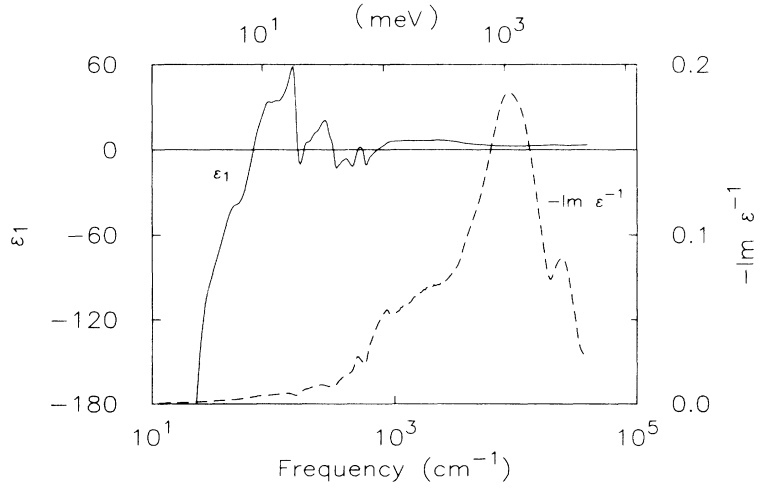

FIG. 2. $\epsilon_1(\omega)$ and $-\mathrm{Im}[\epsilon(\omega)^{-1}]$ for $YBa_2Cu_3O_{7-y}$ as obtained from a Kramers-Kronig analysis of the data in Fig. 1(b). From the solid curve, $\epsilon_1(\omega)$, we obtain the high-frequency limit of the dielectric constant $\epsilon_\infty = 3.7$. The dielectric loss function, $-\mathrm{Im}[\epsilon(\omega)^{-1}]$, shown as the dashed curve, has its peak(s) shifted by 1 to 2 orders of magnitude from the zero crossings of $\epsilon_1(\omega)$.

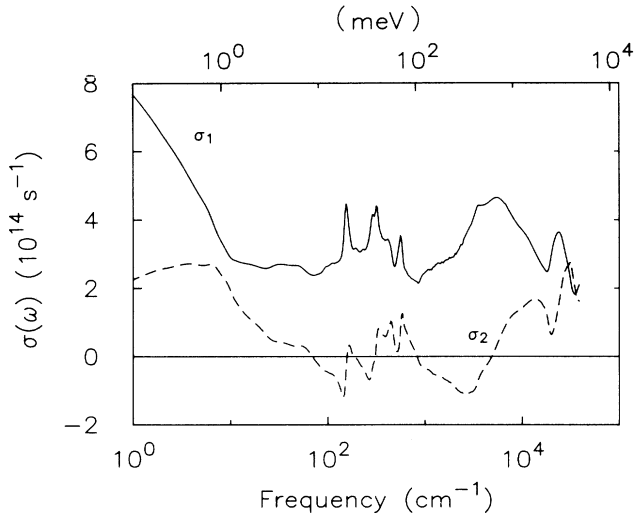

FIG. 3. The real (solid curve) and imaginary (dashed curve) parts of the complex conductivity obtained from the Kramers-Kronig analysis of the reflectivity data in Fig. 1(b). σ_1 rises to the zero-frequency value of 1.1×10^{15} s^{-1}, determined by the low-frequency extrapolation to the data.

We have fit the structures identified with bound carriers (interband transitions and phonons) to the Lorentzian form

$$\sigma_B(\omega)=\sum_j \frac{\Omega_j^2/4\pi}{\gamma_j - i(\omega^2-\omega_{0j}^2)/\omega}\ , \qquad (1)$$

with the parameters shown in Table I. After removing the bound-carrier contribution, the remaining σ_1 is very flat above 10 cm^{-1}, and below this there is the rise to the dc conductivity previously mentioned. If, for the moment, we ignore this rise in the conductivity below 10 cm^{-1} we can get a reasonable Drude fit to the free-carrier data with $\omega_p=4.0\times10^{15}$ s^{-1} (2.6 eV) and $\tau=1.9\times10^{-16}$ s. Since $\omega_p\tau<1$, plasma oscillations are overdamped in this material.

In the FIR the free-carrier response does not resemble that of a regular metal (such as copper). The conductivity, however, can be analyzed in terms of the Drude model with a frequency-dependent relaxation time and effective mass. Taking the conductivity in Fig. 3 and using the notation to describe the complex relaxation frequency $\gamma(\omega)$ found in Ref. 12, we extract forms for the free-carrier relaxation frequency $\mathrm{Re}[\gamma(\omega)]$ and mass enhancement parameter $\lambda(\omega)=-\mathrm{Im}[\gamma(\omega)]/\omega$, which are shown in Fig. 4. The results are highly suggestive of a scattering rate which rises linearly in frequency, followed by a saturation for frequencies larger than 25 cm^{-1}. At low frequencies, $\lambda(\omega)$ shows a logarithmic divergence. By subtracting the bound-carrier contribution from the conductivity shown in Fig. 3, the appearance of the curves in Fig. 4 is improved, with $1+\lambda$ remaining positive at all frequencies (as shown by the dashed line) and the real part of the scattering rate remaining constant to the uv region.

Assuming our value of ω_p and the optical band mass to have the free-electron value, we estimate a mean free path from the high-frequency saturation value of the scattering rate to be $\sim$1.2 Å, which is about the same as the Cu-O distance. Thus the saturation of the scattering rate appears as a natural consequence of the unitarity limit constraints.

Such a frequency-dependent scattering rate provides one explanation for the temperature independence of the reflectivity. If the optical scattering rates have reached the saturation value (which is temperature independent) for the range of frequencies measured, then so have the

TABLE I. Parameters used to fit bound-carrier contribution to the conductivity using the Lorentzian form.

ω_0 (cm^{-1})	γ_B (cm^{-1})	Ω (meV)
156	18	55
288	27	48
320	32	59
559	66	88
5420	8660	1460
25000	10440	1480

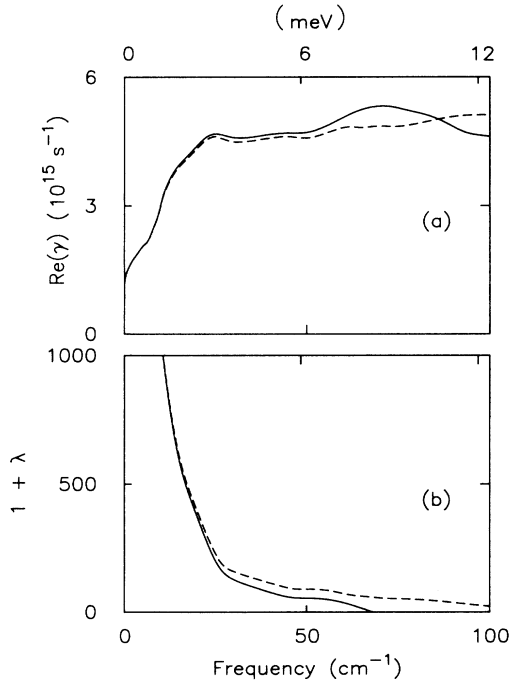

FIG. 4. FIR frequency-dependent parameters describing the free-carrier behavior $YBa_2Cu_3O_{7-y}$. (a) Solid line: the frequency dependent scattering rate $\mathrm{Re}[\gamma(\omega)]$ as obtained from the complex conductivity shown in Fig. 3. Dashed line: obtained after subtracting the bound carriers from the conductivity. (b) Solid line: the mass enhancement $1+\lambda(\omega)$, demonstrating the logarithmic divergence at low frequency. This parameter is driven negative at frequencies above 50 cm^{-1} by the bound contributions. Dashed line: result after bound contributons are subtracted off.

reflectivities, independent of the temperature dependence of the dc scattering rate. On the other hand, the dc resistivity may not provide intrinsic information about the sintered material. Highly conducting grains separated by regions of lower conductivity can produce dispersion at audio frequencies[18] so that a dc measurement may be monitoring an extrinsic property which is unrelated to the optical properties.

Our FIR results, which are independent of an audio frequency extrinsic process, show that the free-carrier conductivity in the normal state has an unusual form which is well fit with a complex frequency-dependent scattering rate. The signature of this scattering is compatible with recent calculations for a 2D square lattice[8-10] which give a scattering rate linear in T and ω for these materials with an attendant logarithmic divergence of the mass enhancement at low frequency.

Work by P.E.S., T.W.N., J.T.M., and A.J.S. is supported by National Science Foundation (NSF) Grant No. DMR-84-09823 and by the U.S. Army Office under Grant No. DAAL03-86-K-0103; work by S.E.R. and R.A.B. by the Office of Naval Research under Grant No. N00014-K-0296; and work by C.S.J., J.E.C., R.E.S., and G.M. by NSF Grant No. DMR-82-19782. One of us (P.E.S.) was partially supported by AT&T Bell Laboratories.

[1]C. M. Varma, S. Schmitt-Rink, and E. Abrahams, Solid State Commun. **62**, 681 (1987).
[2]V. Z. Kresin, Phys. Rev. B **35**, 8716 (1987).
[3]J. Ruvalds, Phys. Rev. B **35**, 8869 (1987).
[4]P. W. Anderson, Science **235**, 1196 (1987).
[5]P. H. Hor *et al.*, Phys. Rev. Lett. **58**, 1891 (1987).
[6]L. Mattheis and D. R. Hamann, Solid State Commun. (to be published).
[7]S. Massidda, J. Yu, A. J. Freeman, and D. D. Koelling, Phys. Lett. (to be published).
[8]J. E. Hirsch, Phys. Rev. B **31**, 4403 (1985).
[9]J. E. Hirsch and D. J. Scalapino, Phys. Rev. Lett. **56**, 2732 (1986).
[10]P. A. Lee and N. Read, Phys. Rev. Lett. **58**, 2691 (1987).
[11]R. J. Cava *et al.*, Phys. Rev. Lett. **58**, 1676 (1987).
[12]B. C. Webb, A. J. Sievers, and T. Mihalisin, Phys. Rev. Lett. **57**, 1951 (1986).
[13]G. A. Thomas *et al.*, Phys. Rev. B **36**, 846 (1987).
[14]F. E. Pinkerton, B. C. Webb, A. J. Sievers, J. W. Wilkins, and L. J. Sham, Phys. Rev. B **30**, 3068 (1984).
[15]L. J. Sham and J. W. Wilkins, Phys. Rev. B **30**, 3062 (1984).
[16]D. Stroud, Phys. Rev. B **19**, 1783 (1979).
[17]D. A. Bonn *et al.*, Phys. Rev. Lett. **58**, 2249 (1987).
[18]C. G. Koops, Phys. Rev. **83**, 121 (1951).